A Mechanism for Forming Large Fluorescent Organo-Silica Particles: Potential Supports for Combinatorial Synthesis

Angus P. R. Johnston,[†] Bronwyn J. Battersby,[†] Gwendolyn A. Lawrie,[†] Lynette K. Lambert,[‡] and Matt Trau*[,†]

Centre for Nanotechnology and Biomaterials, Australian Institute for Bioengineering and Nanotechnology, and Centre for Magnetic Resonance, The University of Queensland, St. Lucia QLD 4072, Australia

Received November 29, 2005. Revised Manuscript Received October 16, 2006

The ability to track multiple compounds through a combinatorial synthesis on solid support particles can be a challenging exercise. A novel solution to this problem is to use the optical characteristics of each support particle to identify the biomolecule synthesized on its surface. To achieve this, we have synthesized a new class of porous, thiol-functionalized supports in a two-step process that used 3-mercaptopropyl trimethoxysilane as the monomer. The monomer was hydrolyzed and polymerized in an acidic solution, which formed an emulsion that was subsequently cross-linked with either ammonia (NH_3) or methylamine (CH_3NH_2). The synthetic process and resulting organo-silica particles were characterized using silicon NMR, scanning electron microscopy techniques, and fluorescence microscopy. Furthermore, thin sections of the porous beads were successfully produced and analyzed via transmission electron microscopy. By controlling the reaction conditions during the synthesis, we achieved a variety of particle morphologies, including hollow particles, particles with macropores on the surface, and particles with a highly porous interior. The mechanism for forming and controlling the morphology of these particles is described here. Also described is the unique process of incorporating fluorescence dyes using combinatorial methods. This enabled the synthesis of a highly optically diverse population of particles, which could be produced over a small number of reactions. Flow cytometry was used to demonstrate the diversity of fluorescence signatures possessed by these encoded particles.

Introduction

For more than a decade, combinatorial chemistry methods have been used to synthesize biologically significant libraries on microscopic solid support particles.[1] However, the challenge, as in all combinatorial chemistry, is keeping track of the multitude of compounds that are synthesized. A number of methods are currently in use to address this challenge,[2] including chemical and magnetic tagging. However, attaching and reading these tags generally involves additional chemical and analytical steps. Moreover, the necessity for compatible compound and tag synthesis reactions places considerable limitations on the procedure.

We have previously outlined an alternative method that makes use of optical codes contained within the support particles in order to track the particles through a combinatorial synthesis.[3] Each support particle possesses a unique optical signature that corresponds directly to the compound attached to the support. The optical signature is generated using a combination of light scattering and fluorescence parameters, and a flow cytometer is used to read the optical code. The diversity of the optical signature is due to the combinatorial incorporation of the fluorescent dyes as well as random orientation of the pores within the particle and slight variations in the particle size.

Using the optical properties of the support particle to encode information places special requirements on the composition of the supports. If these support particles are to be used for combinatorial synthesis (which is a solvent-based method), encoded polystyrene supports are generally not suitable. Organic solvents swell the polystyrene particles and cause the dyes to leach out (because they are typically noncovalently bound), thereby drastically altering the optical signature of the particles. Silica, on the other hand, does not swell significantly in solvents; with fluorescent dyes covalently attached, silica would be an ideal support for use in an encoded combinatorial library. Covalent attachment of dyes is essential as encapsulated dyes, under other circumstances, may leach from the particles during combinatorial synthesis. Commercially available silica particles are either (i) too large and irregularly shaped (e.g., controlled pore glass used in automatic DNA synthesis) for flow cytometric analysis or (ii) nonfunctionalized and cannot be readily encoded with fluorescent dyes.

Silica particles are most commonly synthesized using the Stöber process, and although this method yields monodispersed particles, they are unfunctionalized, nonporous, and have an upper size limit of a few micrometers. Stöber-type particles can be functionalized postsynthesis using organosilanes such as 3-aminopropyl-trimethoxy silane (APS);[4] however, the level of functionalization is limited. Stöber

* Corresponding author. E-mail: m.trau@uq.edu.au. Tel: 61 7 3346 4173, Fax: 61 7 3346 3973.
[†] Australian Institute for Bioengineering and Nanotechnology.
[‡] University of Queensland.

(1) Brenner, S.; Lerner, R. A. *Proc. Natl. Acad. Sci. U.S.A.* **1992**, *89*, 5381.
(2) Czarnik, A. W. *Curr. Opin. Chem. Biol.* **1997**, *1*, 60.
(3) Battersby, B. J.; Lawrie, G. A.; Johnston, A. P. R.; Trau, M. *Chem. Commun.* **2002**, 1435.

10.1021/cm0526260 CCC: $33.50
Published on Web 12/19/2006

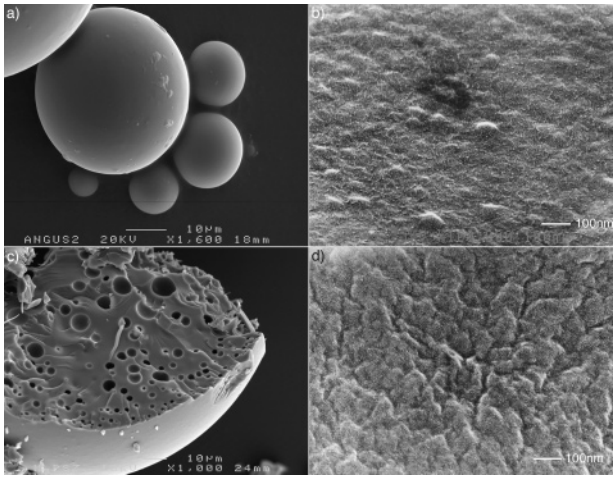

Figure 1. SEM of functionalized porous particles. (a) Particles with a smooth outer surface; (b) high-resolution SEM image showing small pores on the surface of the particle; (c) a fractured particle showing the internal porosity of the particles; (d) high-resolution image revealing fine channels that link the larger pores.

particles have also been synthesized so they contain fluorophores (or a number of fluorophores).[5−10] However, for applications in which a large number of differently coded particles are required, each particle population must be synthesized individually. Additionally, particles synthesized via the Stöber method are typically less than 3 μm in diameter. Particles this small have limited applications for solid-phase synthesis, as they are not retained by the standard filters employed during synthesis.

We recently reported on the development of organo-silica particles that are (i) spherical, (ii) suitable for flow cytometric analysis, (iii) highly porous and functionalized, and (iv) sufficiently large in diameter to be retained by combinatorial chemistry filters.[11] The porosity and functionality permits fluorescent dyes to be covalently incorporated throughout the particle. In the present study, we propose a mechanism for forming these highly functionalized organo-silica particles (Figure 1). The porous particles are synthesized using 3-mercaptopropyl trimethoxysilane (MPS) monomer rather than the more traditional tetraethoxysilane (TEOS), which results in the particles being highly thiol-functionalized. By using MPS, potentially every silica unit can be coupled to a fluorophore (or biomolecule) via the thiol moiety. Because the fluorophores are incorporated into the particles postsynthesis (as opposed to during the hydrolysis and condensation processes, as is the case in a Stöber synthesis), combinatorial techniques can be used to create optically diverse sets of particles while using the minimum number of dye coupling reactions.

Biomolecules may be synthesized on the surface of the particles by functionalizing the particles with an amine group.[4] This allows a wide variety of organic molecules to be synthesized on the support.

Experimental Section

Synthesis. *Particle Synthesis.* Thirty-five percent HCl (110 μL) was placed in 10 mL of water (MilliQ, Millipore) to form a 0.1 M solution. Eight hundred microliters of this solution was added to 80 mL of water with 10 mL of MPS (3-mercaptopropyl trimethoxysilane, Aldrich). The solution was stirred at 2000 rpm for 48 h.

Twenty-five percent ammonia solution (8 mL, Sigma Aldrich) was added to 100 mL of H_2O ($\sim$1 M), and the 48 h old MPS solution was slowly added. The experiments were conducted while the catalyst solutions were quiescent. Immediately after addition of catalyst, the MPS reaction vessel was rinsed with $\sim$75 mL of ethanol (Ajax), which was added to the ammonia−MPS solution. The addition of ethanol after the addition of the catalyst was necessary to slow the formation of undesired Stöber-like particles that form when unpolymerized monomer in the aqueous phase reacts with the ammonia. After the addition of the ethanol, the mixture was filtered in a Buchner funnel under a vacuum using type 13 filter paper (Whatman). The particles collected were rinsed with ethanol, collected from the filter, and then resuspended in 3 mL of ethanol. The particles synthesized covered a broad size range (from 5 to 50 μm). To separate the different sized particles, nylon net filters (MilliPore) of different mesh size (11, 20, 30, and 60 μm) were used. The majority of particles synthesized were in the 11−20 μm and <11 μm size fraction. The particles used for fluorescence staining were in the <11 μm size fraction.

The same procedure was repeated for the other concentrations of ammonia (0.14, 2.7, and 6.7 M) and methylamine (2.7 and 6.7 M). When 0.14 M ammonia was used to cross-link the emulsion, the solution was allowed to stand for 5 min before the ethanol was added. This was to ensure that the cross-linking of the emulsion was complete. The addition of ethanol immediately after the addition of the ammonia did not result in the formation of particles.

Postsynthesis Dye Modification. Fluorescent dyes (Alexa Fluor 350 isothiocyanate (λ_{ex} = 346 nm, λ_{em} = 445 nm), Oregon Green isothiocyanate (λ_{ex} = 495 nm, λ_{em} = 521 nm) and carboxytetramethylrhodamine isothiocyanate (TAMRA; λ_{ex} = 542 nm, λ_{em} = 568 nm; Molecular Probes) were incorporated into the particles by simply placing the particles into the supernatant of saturated solutions of these dyes in tetrahydrofuran (THF, Sigma Aldrich). The particles were washed at least three times in ethanol to remove excess dye. To form optically diverse particles, a split and mix process was used. Twenty microliters of particles (200 000 particles per μl) were placed in six Eppendorf tubes. Fifty microliters of Alexa Fluor 350 with varying concentration (0, 300, 500, 700, 900, and 1000 nM) was added, and the particles were allowed to react. After 90 min, the particles were washed 4 times in THF. After the first wash, the particles were combined in the same tube. The particles were resuspended in 300 μL of THF, and the solution was evenly divided into another six Eppendorf tubes. This split-and-mix combinatorial process was repeated using varying concentrations of TAMRA and then Oregon Green dyes.

Methods

NMR Spectroscopy. Solution NMR analysis was performed using a 5 mm broadband probe on a Bruker AV400 spectrometer observing ^{13}C at 100.618 MHz and ^{29}Si at 79.491 MHz. Spectra were acquired without lock of 1 mL aliquots of the bead reaction mixture after 2 h and after 24 h of mixture preparation.

(4) Gellermann, C.; Storch, W.; Wolter, H. J. *Sol−Gel Sci. Technol.* **1997**, *8*, 173.
(5) Van Blaaderen, A.; Vrij, A. *J. Non-Cryst. Solids* **1992**, *149*, 161.
(6) Imhof, A.;Megens, M.; Engelberts, J. J.; de Lang, D. T. N.; Sprik, R.; Vos, W. L. *J. Phys. Chem. B* **1999**, *103*, 1408
(7) Matthews, D. C.; Grondal, L.; Battersby, B. J.; Trau, M. *Aust. J. Chem.* **2001**, *54*, 649.
(8) Van Blaaderen, A.; Vrij, A. *J. Colloid Interface Sci.* **1993**, *156*, 1.
(9) Van Blaaderen, A.; Vrij, A. *Langmuir* **1992**, *8*, 2921.
(10) Lawrie, G. A.; Battersby, B. J.; Trau, M. *Adv. Funct. Mater.* **2003**, *13*, 887.
(11) Johnston, A. P. R.; Battersby, B. J.; Lawrie, G. A.; Trau, M. *Chem. Commun.* **2005**, 1435.

Proton-decoupled carbon spectra were acquired over a spectral width of 17 100 Hz using a 30° pulse and a recycle time of 2.4 s. We accumulated 460 scans, and the fid was zero-filled prior to transformation to give a final digital resolution of 0.26 Hz.

After running the initial ^{13}C NMR spectrum on the 2 h sample, we added 50 μL of methanol and acquired the spectrum. The methanol signal was coincident with the lowest field peak in the reaction mixture, and this signal was used as the reference for the ^{13}C spectrum (49 ppm).

^{29}Si spectra were acquired using the DEPT sequence.[12] The spectra were acquired with the τ delay set for $^2J_{Si-H} = 9.5$ Hz, and the final proton observation pulse width was optimized for 2-coupled protons.[13] ^1H composite pulse decoupling was switched on during the acquisition time. For the 2 h aliquot, 270 scans were acquired with a spectral width of 15 000 Hz using an acquisition time of 2.2 s and an additional relaxation delay of 1.5 s. A line-broadening of 0.8 Hz and zero-filling was applied to the spectra before transformation to give a final digital resolution of less than 0.3 Hz. Similar conditions were used for the 24 h aliquot except that 2000 scans were acquired over a spectral width of 8700 Hz. ^{29}Si spectra were referenced to TMS (0 ppm) for a sample of TMS in $CDCl_3$ in a separate NMR tube.

The ^{29}Si solid-state spectrum was run on a Bruker MSL300 spectrometer operating at 300.13 MHz for ^1H and 59.627 MHz for ^{29}Si. Experiments were performed with a standard Bruker 7 mm MAS probe. The MAS spinning speed was 2 kHz. The 90° pulse time for both ^1H and ^{29}Si was 6.8 μs. The spectra were recorded using the standard pulse and collect sequence with a recycle delay of 15 s and high-power proton decoupling during acquisition. The spectral width was 60.24 kHz, and 2000 data points were collected. On processing, a line broadening of 50 Hz was used.

Scanning Electron Microscopy. The particles were suspended in ethanol and deposited on glass cover slips attached to carbon stubs. A platinum splutter coat was applied before the samples were examined on a JEOL 6400 FE SEM. High resolutions scans were obtained on a JEOL 630 FE SEM using an accelerating voltage of 5 keV.

Transmission Electron Microscopy. The particles were suspended in LR White resin (Proscitech) and cured at 60 °C for 20 h before microtome sectioning (Ultracut E) to approximately 80 nm using a 45° diamond knife. These sections were mounted on Formvar-coated copper grids (Proscitech) and examined on a JEOL 1010 transmission electron microscope. Images were obtained at an accelerating voltage of 80 keV.

Bright-Field Microscopy. The cross-linking reaction during the formation of the particles was observed and recorded on an Olympus IX70 inverted microscope. A drop of catalyst solution was added to the acid hydrolyzed emulsion on a microscope slide. Real-time images were recorded using a 10× objective lens and a JVC EEC CCD video camera.

Fluorescence Microscopy. Fluorescence microscopy images of the particles were obtained using a SPOT Diagnostic Instruments camera mounted on an inverted microscope (Olympus IX70). A mercury lamp was mounted on the microscope as an excitation source, and the microscope was equipped with three filters: U-MWU ($\lambda_{ex} = 330-385$ nm, $\lambda_{em} > 420$ nm), U-MWB ($\lambda_{ex} = 450-480$ nm, $\lambda_{em} > 525$ nm), and U-MWG ($\lambda_{ex} = 510-550$ nm, $\lambda_{em} > 590$ nm). Images were analyzed using Image Pro-plus 4.0 software.

Flow Cytometry. The fluorescence characteristics of the particles were determined using a high-performance flow cytometer (MoFlo, DakoCytomation, USA). The fluorescent dyes incorporated within the particles were excited by one of three lasers: an argon-ion water-cooled laser (I90C, Coherent Scinetific, Australia) at 100 mW producing both a 488 nm line and a 351 nm line. The third laser was a 635 nm red diode laser excitation source. Emission profiles were recorded in the linear mode using the 530/30, 580/30, and a 630/30 nm bandpass filters.

Results and Discussion

The method for preparing the organo-silica support particles comprised a two-step process that initially involved acid-catalyzed hydrolysis, followed by base-catalyzed cross-linking of the emulsion. Initially, MPS monomer was added to an acidic solution, where it formed an emulsion upon stirring. Under acidic conditions, the insoluble MPS monomer quickly hydrolyzed to form solubilizing silanol groups. This was evident as the emulsion gradually broke down to give a clear solution. The hydrolysis was confirmed using ^{13}C NMR (see the Supporting Information).

As in the Stöber process using TEOS, a condensation reaction occurs after the hydrolysis of the silane monomer (Figure 2a). In the process described here, the thiol functionalized monomer has three reactive sites for condensation, rather than four. As the condensation reaction proceeds, short polymer chains are formed. The four possible silane centers (Figure 2a) may be observed using ^{29}Si NMR spectroscopy (Figure 2b−d). ^{29}Si NMR gives a clear separation of the silica species present, with the chemical shift of the Si atom shifted by approximately 10 ppm to higher field[8,14,15] with each subsequent condensation reaction. The ^{29}Si NMR spectrum (Figure 2b) of a sample treated with acid for 2 h shows the presence of only the monomer (T_0) at −39 ppm and dimer (T_1) at −48 ppm, confirming that no significant condensation of the monomer had occurred after 2 h. This indicates a slow condensation rate of the monomer, probably because the pH of the aqueous solution (the pH of the solution changes as hydrolysis proceeds, but stays in the range of pH 2−3) is close to the isoelectric point of the monomer (estimated to be around pH 3).[17] The condensation of silanols above the isoelectric point occurs by the reaction between a deprotonated silanol and a silicic acid monomer.[16] Below the isoelectric point, a lone pair of electrons on a silicic acid monomer can attack the Si center of a protonated silanol. At the isoelectric point, the condensation rate is at a minimum because neither reaction mechanism is favored.[17]

As the polymerization reaction proceeds, the solution gradually becomes cloudy, with an emulsion once again being formed. The emulsion is due to the presence of short polymer chains (oligomers), which are formed from the slow polymerization of the monomer. The oligomers are not soluble in the aqueous phase; however, as an oily liquid, they form an oil-in-water emulsion.

The presence of short linear polymer chains in the emulsion can be observed in the ^{29}Si NMR after 24 h (Figure

(12) Pegg, D. T.; Doddrell, D. M.; Bendall, M. R. *J. Chem. Phys.* **1982**, *77*, 2745
(13) Doddrell, D. M.; Pegg, D. T.; Brooks, W.; Bendall, M. R. *J. Am. Chem. Soc.* **1981**, *103*, 727.
(14) Brus, J.; Karhan, J.; Kotlik, P. *Collect. Czech. Chem. Commun.* **1996**, *61*, 691.
(15) Delattre, L.; Dupuy, C.; Babonneau, F. J. *Sol−Gel Sci. Technol.* **1994**, *2*, 185.
(16) Fyfe, C. A.; Aroca, P. P. *Chem. Mater.* **1995**, *7*, 1800.
(17) Iler, R. K. *The Chemistry of Silica*; Wiley: New York, 1979.

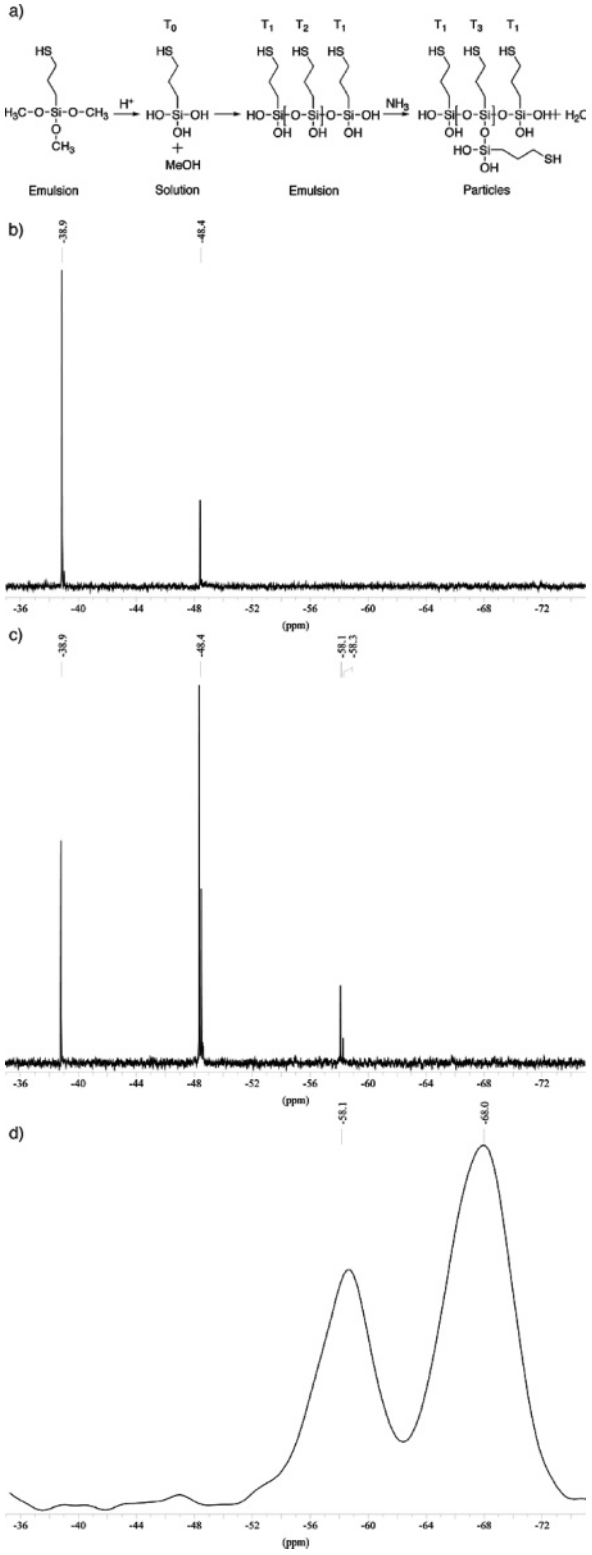

Figure 2. Condensation mechanism and NMR. (a) Hydrolysis and condensation of 3-mercaptopropyl trimethoxysilane (MPS). There are four possible silane centers that may be observed in ^{29}Si NMR spectra. The nomenclature of the peaks has been standardized[18] using a T to denote that there are three potential sites on the silane that could condense and a subscript number indicating the number of times the silane center has condensed. (b) ^{29}Si NMR spectrum after 2 h of acid-catalyzed hydrolysis of MPS showing the presence of the monomer (T_0) at −39 ppm and the T_1 species at −48 ppm. (c) After 24 h, ^{29}Si NMR spectroscopy shows peaks at −39, −48, and −58 ppm, indicating the presence of monomer (T_0), T_1, and T_2 species, respectively. There is a clear drop in the intensity of the T_0 peak from the 2 to the 24 h sample. (d) ^{29}Si Solid-state NMR after cross-linking with 2.7 M ammonia. The T_2 and T_3 centers are the predominant species present.

2c). The NMR after 24 h clearly shows a decrease in monomer (T_0) and a marked increase in the T_1 and T_2 species. For each type of condensed silica (T_1, T_2, and T_3), small changes in chemical shift indicate a different chemical environment and give an indication of the length of the oligomer chains. For example, small chemical shift differences occur for the T_1 centers present in dimers and trimers.

In the 24 h ^{29}Si NMR sample (Figure 2c), there are four T_1 peaks present. The peak at lowest field (−48.39 ppm) is due to a simple dimer, and a lower intensity peak at −48.52 ppm is due to the terminal Si of a trimer. The very low intensity peaks at −48.61 and −48.70 ppm indicate the presence of longer chains. Two peaks are present in the T_2 region: the peak at −58.16 ppm is due to the central Si of a trimer and the lower-intensity peak at −58.24 ppm is due to a longer chain component. It is probable that longer polymer chains are present in the oil phase of the emulsion but not detected within the sensitivity of the liquid-state NMR experiment. We propose several reasons for this observation. As the lengths of polymer chains increase, the transverse relaxation times (T_2) decrease,[19] and NMR signals broaden. Relatively more signal is lost during the length of the DEPT pulse sequence[12] for compounds with short T_2 values. The viscosity of the oil phase is higher than that of the aqueous phase, leading to slower molecular tumbling and, therefore, shorter T_2 values. Additionally, some settling out of the oil droplets to the base of the NMR tubes occurred in the spectrometer probe during spectral accumulation.

If the solution is allowed to polymerize for more than 3 days, a white debris is formed at the bottom of the reaction vessel that, although insoluble in the aqueous phase of the reaction mixture, dissolves readily in ethanol. This is likely to be due to the formation of longer polymer chains, which cannot form stable emulsion droplets and aggregate at the bottom of the reaction vessel.

Stable, solid particles were formed by adding a cross-linking catalyst (ammonia, or another water-soluble amine[20]) to the emulsion. When the catalyst was added, dark spots appeared within the emulsion droplets, and these dark spots were observed to swirl around until the cross-linking process was complete (Figure 3).

When the condensation catalyst in the aqueous phase reaches the surface of the oil droplet, it starts to catalyze the cross-linking between the silicon oligomers at the surface of the droplet. A byproduct of the condensation reaction is water, which is not soluble within the emulsion droplet. The water produced from the condensation reaction coalesces to form a water-in-oil-in-water double emulsion. It is proposed that the water droplets are swirled around because, as the oligomers at the surface of the silica droplets condense, oligomers from the center of the particle migrate to the surface to combat the concentration gradient which is formed.

The longer the emulsion is hydrolyzed in acid before the cross-linker catalyst is added, the slower the motion of the

(18) Brinker C. J.; Scherer, G. W. *Sol−Gel Science: The Physics and Chemistry of Sol−Gel Processing;* Academic Press: London, 1990.
(19) Grant, D. M.; Harris, R. K. *Encyclopedia of Nuclear Magnetic Resonance Spectroscopy*; John Wiley and Sons Ltd.: Chichester, U.K., 1996; Vol. 6, p 3988.

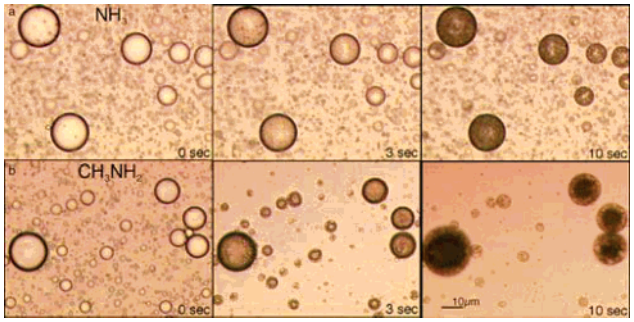

Figure 3. Particle formation from emulsion droplets. Brightfield microscopy images showing the formation of water droplets within the emulsion droplets after the addition of the cross-linking catalyst. (a) Images taken at 0, 1, 3, 5, and 10 s after the addition of 2.7 M ammonia solution. (b) Images taken at 0, 1, 3, 5, and 10 s after the addition of 2.7 M methylamine solution. Note the swelling of the particles in the final 5 s.

water droplets inside the emulsion after addition of catalyst. The polymer chains present in the older droplets are longer, and therefore the oil is more viscous (unpublished data). Consequently, when the concentration gradient is formed, it is more difficult for the polymer chains to migrate to the surface of the emulsion droplet, and thus the water droplets move more slowly. The viscosity reaches a point, as observed in the 3-day-old sample, where it is so high that the water droplets formed do not appear to swirl at all. In these samples, it is proposed that the cross-linker diffuses through the particle, cross-linking the particle from the external surface toward the core.

The formation of water in the particles results in macropores and microchannels being formed within the particles (Figure 1), ranging in size from less than 1 μm to more than 10 μm, depending on the reaction conditions. These large pores are evenly but randomly distributed throughout the particles. They are interconnected via a network of fine channels that are around 30 nm in diameter (Figure 1d) causing the particles to be quite highly porous.

Solid-state ^{29}Si NMR spectroscopy[21] confirmed the emulsion droplets had been condensed to form highly cross-linked particles (Figure 2d) after exposure to the condensation catalyst. Although the resolution of solid-state NMR spectroscopy is inherently poorer than solution-phase NMR spectroscopy, the distinction between the T_1, T_2, and T_3 silica peaks was still clearly apparent. As expected in the solid sample, no significant peak due to the monomer (T_0) or the least condensed silica (T_1) was observed. The most significant peaks in the spectrum are due to the most condensed silica species (T_3, -68 ppm) and the T_2 peak (-58 ppm).

Catalyst species and concentration appear to significantly affect the cross-linking rate and the size of pores within the particles. Figure 4 shows the morphological changes that occurred upon cross-linking with different ammonia concentrations. The use of low catalyst concentrations (0.14 M) typically results in poorly cross-linked particles with large pores on the outer surface (Figure 4a). The cross-linking of the emulsion droplet is slow because of the low availability of catalyst. The slow rate of cross-linking allows the water

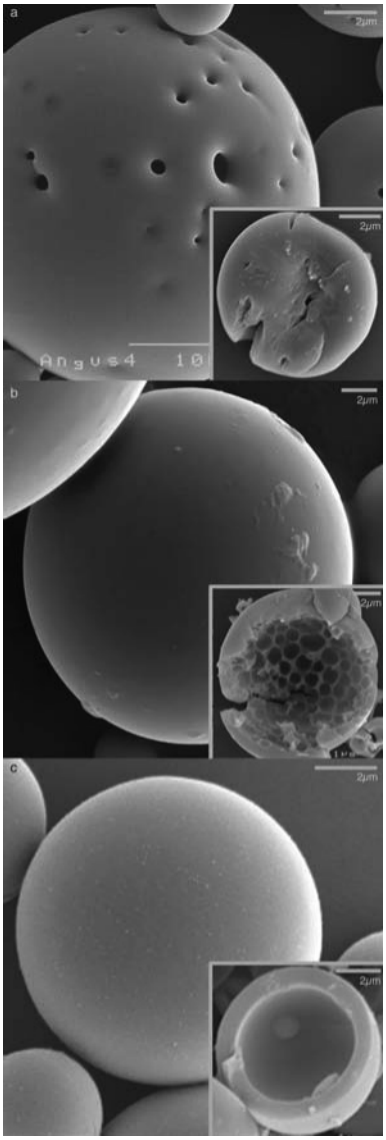

Figure 4. Scanning electron microscopy images of cross-linked functionalized silica particles. (a) Particles synthesized with a low (0.14 M) ammonia concentration showing large surface pores and a crushed particle (inset) showing that the particles have a rubbery texture. (b) Particle synthesized with the optimal ammonia concentration (2.7 M) and a fractured particle (inset). (c) Hollow particles formed by cross-linking with high ammonia concentration (6.7 M), fractured particle (inset).

formed within the emulsion droplet to migrate to the outer surface and escape into the aqueous reaction mixture, before the outer surface has completely solidified. Consequently, large pores were evident on the outer surface of the cross-linked particle. An increase in catalyst concentration appeared to increase the rate of cross-linking, so at higher concentrations, the outer surface of the emulsion droplet solidified quickly, forming particles with a smooth surface (Figure 4b). The particles formed at the highest concentration of catalyst (6.7 M) were hollow. When a small amount of force was applied to the particles, the particle fractured cleanly around the circumference particle, revealing an outer shell approximately 1 μm thick (measured by SEM, Figure 4c).

Whereas most condensation catalysts, such as ammonia, trimethylamine, and triethylamine, behaved similarly, methylamine performed quite differently. At the same concentration as the other amines, methylamine induced formation of

(20) Mizutani, T.; Nagase, H.; Fujiwara, N.; Ogoshi, H. B. *Chem. Soc. Jpn.* **1998**, 71, 2017.
(21) Stöber, W.; Fink, A.; Bohn, E. *J. Colloid Interface Sci.* **1968**, *26*, 62.

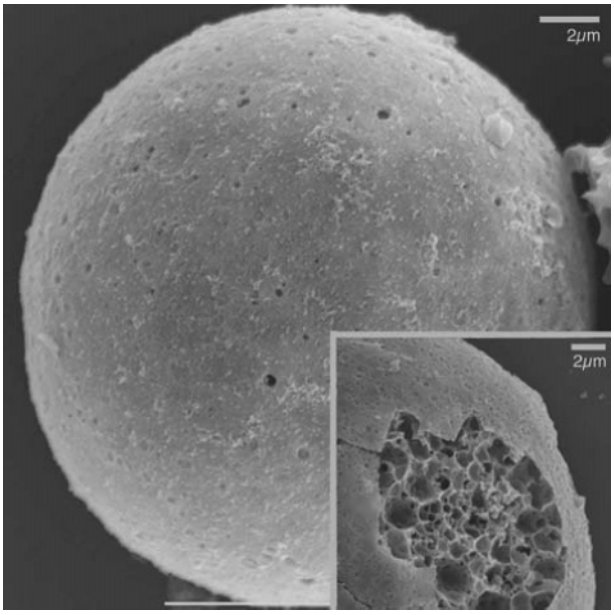

Figure 5. SEM image of a methylamine cross-linked particle. Particle after cross-linking with methylamine (4 M) and (inset) showing oval-shaped pores that are formed on the outer region of particles as a result of particle swelling during cross-linking.

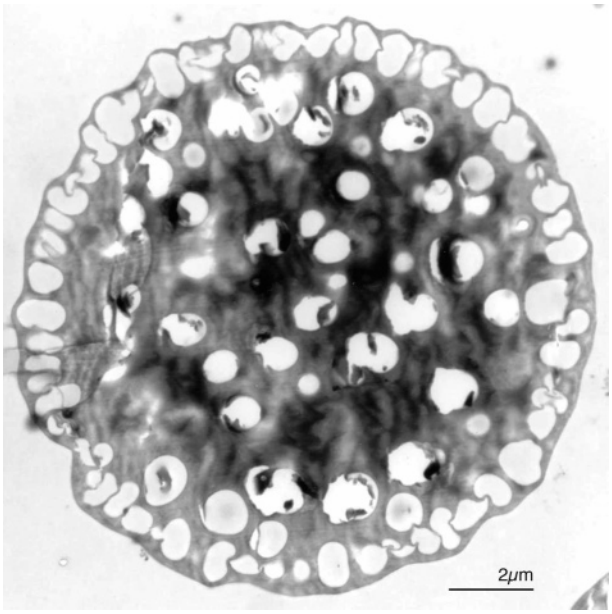

Figure 6. TEM cross-section of a particle. The cross-sectional TEM image of a particle cross-linked with 2.7 M methylamine solution showing large pores distributed throughout the particle. Also visible are elongated pores at the edge, formed by swelling of the particle in the final stages of solidification (see also Figures 3b and 5).

some very large droplets as well as many significantly finer droplets within the large silica emulsion drops (Figure 3b), instead of forming water droplets within the double emulsion that were all a similar size (as with the other catalysts used). After the cross-linking process appeared to be complete, a secondary process occurred in which the large particles swelled significantly. SEM of the particles showed highly porous surface of the particles (Figure 5), and cross-sections of a fractured particle showed the swollen surface pores (Figure 5, inset, and Figure 6). The swelling of the particle was possibly due to the methylamine cross-linking the surface of the particle very quickly and forming a semirigid

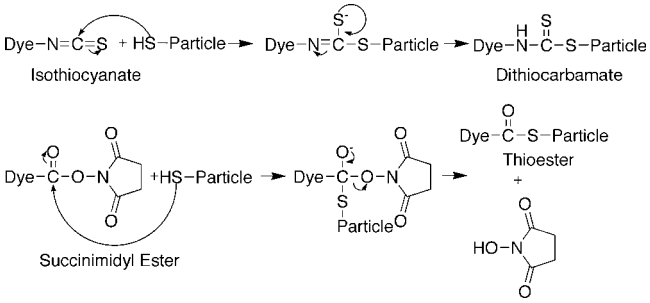

Figure 7. Mechanism of the reaction of an isothiocyanate and a succinimidyl ester-modified dye with the thiol functionalities throughout the silica particles.

balloonlike skin on the surface of the droplet. It is believed that the difference in density of the short polymer chains and the condensed silica plus water generates a gradual build up of pressure within the particle, eventually forcing the surface skin to expand.

Incorporation of Fluorescent Dyes. There are a variety of methods for encoding silica particles with fluorescent dyes. It is known that through a modification of the Stöber process,[9] silane coupling agents, such as aminopropyl trimethoxysilane (APS), can react with functionalized fluorescent dyes and then be covalently incorporated into the silica matrix of the particles.[10] Furthermore, silica shells containing different fluorescent material can be synthesized onto the particles to increase the optical diversity.[18] However, the fluorescent dyes must be incorporated into the particle during the shell synthesis. In an alternative system, the dyes can be covalently coupled to the particles post-particle synthesis in a way that allows flexible incorporation of multiple dyes. The porous nature of the particles described in this article promotes the absorption of organic compounds such as fluorescent dyes within their structure, offering a versatile approach to manipulating their optical properties. The thiol functionality enables the covalent attachment of isothiocyanate-, maleimide-, or succinimidyl ester-functionalized fluorescent dyes to the particles, which prevents dyes from leaching (Figure 7). The extent of this diversity can be seen in flow cytometry and fluorescence microscopy studies.

By incorporating dyes into the particles in a combinatorial split-and-mix manner (using three different dyes and six different dye concentrations), we produced particles displaying a diverse range of optical signatures (Figure 8). Figure 8a shows that by plotting the green fluorescence (Oregon Green, 510-550 nm) vs red fluorescence (TAMRA, 565-595 nm) intensity collected from two different detectors on a flow cytometer, it was possible to cover almost the entire parameter space with the optically diverse population of particles.

The fluorescence microscopy image of a split-and-mix set of particles using three fluorescent dyes (AlexaFluor 350, Oregon Green and TAMRA) gives a visual indication of the diversity that can be achieved with a small number of dyes. Figure 8b indicates that there is a slightly larger number of particles with lower fluorescence intensity. This is a product of the nature of the particles; however, it does not effect the ability to use the fluorescence signature as a code. Figure 8c shows the diversity covering the entire three-dimensional

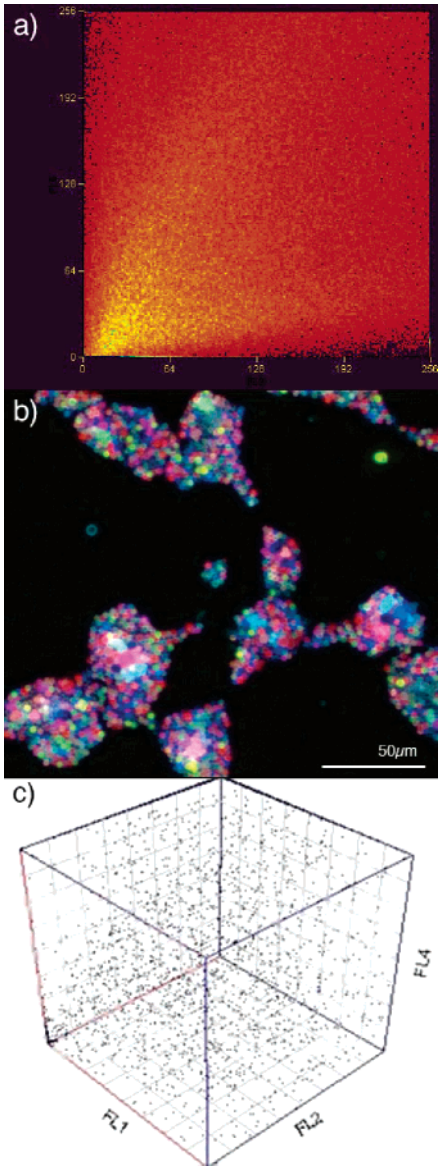

Figure 8. Optical diversity of functionalized organosilica particles after incorporation of fluorescent dyes. (a) Flow cytometry data showing the orange fluorescence emission vs green fluorescence emission. Each point on the plot represents a single particle, and the high degree of diversity is shown by the set of particles covering the entire optical space. (b) Fluorescence micrograph showing the optical diversity achieved by incorporating three dyes in a combinatorial split-and-mix fashion. (c.) Three-dimensional plot of flow cytometry data showing the optical diversity in three dimensions (FL1, 510-550 nm; FL2, 565-595 nm; FL4, 440−480 nm).

space. The number of unique particles that can be encoded is limited by the reproducibility of the fluorescence signal from the particles (which is a product of the resolution of the flow cytometer and the variation of the position of the particles in the flow cytometer stream). Typically, eight levels of fluorescence intensity (as shown here) from each parameter can be achieved. Only three parameters are shown in this example; however, the optical signature can extend into many other parameters depending upon the number of fluorophores used to dye the particles.

The significance of this outcome is that the enormous number of particles, each possessing a unique fluorescence signature, shown in Figure 8 have the potential to each be tracked through multiple passes using the high-performance flow cytometer. The unique fluorescence signature enables both tracking and direction of the particles into sorted populations of particles, which can then be used for any application of a library of species. They are both chemically and photo stable and subsequent exposure to solvents during the synthesis of probe molecules on the surface of the particles becomes viable. The major application of these particles is in the directed combinatorial synthesis of peptide and oligonucleotide libraries in genomics and proteomics research.

Conclusions

Proposed here was the mechanism of formation of novel functionalized silica particles. Varying the concentration and type of cross-linking catalyst resulted in particles that exhibited different internal and external morphologies and porosities. The particles were both highly functionalized and porous, which allowed fluorescent dyes to be covalently incorporated into the particles to form an optical barcode. Being able to resist swelling and dye leaching, these functionalized particles have great potential as solid supports for optically encoded combinatorial library synthesis and biomolecular screening applications.

Acknowledgment. This work was supported by the Australian Research Council (FF0455861). The authors thank the Nanomics BioSystems Pty. Ltd. for A.P.R.J.'s industry scholarship. We gratefully acknowledge the NHMRC and Nanomics BioSystems for NHMRC Industry Fellowship support for B.J.B. (NHMRC application 301267). We would also like to acknowledge the Centre for Microscopy and Microanalysis and the Centre for Magnetic Resonance at the University of Queensland.

Supporting Information Available: ^{13}C NMR spectra. This material is available free of charge via the Internet at http://pubs.acs.org.

CM0526260